Dynamical properties of inertial confinement fusion plasmas

S.K. Kodanova | **T.S. Ramazanov** | **A.K. Khikmetov** | **M.K. Issanova**

IETP, Al-Farabi Kazakh National University, Almaty, Kazakhstan

*Correspondence
M.K. Issanova, IETP, Al-Farabi Kazakh National University, Al-Farabi 71, Almaty 050040, Kazakhstan.
Email: moldir.issanova@gmail.com

In this paper, we calculate the stopping power and temperature relaxation of dense plasmas on the basis of the Coulomb logarithm using the effective potentials. These potentials take into account long-range multi-particle screening effects and short-range quantum mechanical effects in two-temperature plasmas. Ion energy losses in the plasma for different values of temperature and plasma density are calculated. The obtained results are compared with the theoretical works of other authors and with the results of molecular dynamics simulations.

KEYWORDS
Coulomb logarithm, dense plasma, effective potentials, inertial confinement fusion, stopping power

1 | INTRODUCTION

Investigation of the interaction processes of ion beams with dense plasmas is one of the most important problems in the physics of inertial confinement fusion (ICF), warm dense matter, and high-power laser physics.[1–3] The dense plasma is formed in the experiments on heavy ion-driven fusion,[4–6] experiments at the National Ignition Facility,[7] and magnetized Z-pinch experiments.[8] Currently, a large number of theoretical[9–14] and experimental studies of physical processes that determine the design of the thermonuclear target are carried out. The study of energy losses of charged particles in the plasma is of great importance for dense plasma physics, as well as for solution of the problems of inertial fusion.[15,16] The nature and results of these interactions depend on the type of energy of the charged particle beam as well as on the type, condition, density, composition, and size of the targets. Therefore, modelling of heavy, highly charged ions for inertial thermonuclear fusion requires both qualitative and quantitative description of the interaction of heavy particles with matter in a wide range of densities and temperatures. It is especially important to determine ion energy losses in dense plasmas, as their experimental study has certain difficulties related to the determination of free-electron density in the plasma needed for calculation of their stopping power. The stopping power has been calculated in many theoretical works using various approaches, theories, and computational simulations.[17–20] It was found that, in general, the stopping power increases in two cases, that is, when the effective charge of the projectile increases, and when the value of the Coulomb logarithm increases. The traditional formula for the Coulomb logarithm does not correctly account for collisional processes in systems, because it is obtained by using an unscreened Coulomb potential. In this work, the Coulomb logarithm is derived on the basis of a strongly screened effective potential, which accounts for short-range quantum effects and long-range many-particle screening effects.

In this paper, the model previously proposed in Refs [21–24] for the description of dense plasma properties based on effective interaction potentials[25–27] is used for calculation of the dynamical properties of deuterium–tritium ICF plasmas. The effective potential is derived using the long-wavelength expansion of the polarization function and quantum potential, taking into account the finite value of the interaction potential at a close distance.

In Section 2, we present the model for the calculation of the dynamical properties of the dense plasma using effective potentials of the electron–ion interaction. In Section 3, we present and discuss the results of calculation of the stopping power and temperature relaxation of the ICF plasma. To show the correctness of the model, its results are compared with the data from molecular dynamics (MD) and particle-in-cell (PIC) simulations. In the last section, the findings are summarized.

2 | PHYSICAL MODEL

The basis of controlled nuclear fusion is to provide a fusion reaction of light nuclei. In the thermonuclear fusion of deuterium and tritium, $D + T \rightarrow \alpha + n$, which occurs in ICF experiments, the amount of the initial α-particle energy, $E_0 = 3.54$ MeV, transferred to the D and T ions is crucial because a high ion temperature is needed for the fusion reaction parameter $\langle \sigma v \rangle_T$ to become sufficiently large so that a robust and stable fusion burning can be realized. The range of particles is determined as follows:[28]

$$R = \int_{\bar{E}}^{E_0} \left(\frac{dE}{dx} \right)^{-1} dE, \tag{1}$$

where dE/dx is the stopping power, E_0 is the initial energy of the particle, and $\bar{E}$ is determined from the condition $S(\bar{E}) = dE/dx = 0$. If the projectile moves linearly through the plasma until it stops, the energy partition into ions and electrons is given by[29]

$$E_i = \int_0^{E_i} dE_i = \int_0^{E_0} dE \frac{dE_i/dx}{dE/dx}, \tag{2}$$

$$E_e = \int_0^{E_e} dE_e = \int_0^{E_0} dE \frac{dE_e/dx}{dE/dx}, \tag{3}$$

where dE_i/dx and dE_e/dx are the stopping power contributions from ions and electrons, respectively, and dE/dx is the total stopping power:

$$\frac{dE_i}{dx} + \frac{dE_e}{dx} = \frac{dE}{dx}, \tag{4}$$

$$E_i + E_e = E_0. \tag{5}$$

In this paper, the dynamical properties are obtained on the basis of the Coulomb logarithm using the effective potentials for an ICF plasma. Stopping power is defined as the average energy loss per unit path length of charged particles passing through the material due to Coulomb interactions with electrons or ions. We calculate the stopping power in the binary collision approximation,[30,31] as

$$\frac{dE_\alpha}{dx} = 8\pi n \left(\frac{m_{\alpha\beta}}{m_i} \right) \cdot E_c \cdot b_\perp^2 \cdot \Lambda_{\alpha\beta}, \tag{6}$$

where α and β stand for the types of colliding particles, $E_c = \frac{1}{2} m_{\alpha\beta} v^2$ is the energy of the center of mass of the colliding particles, $m_{\alpha\beta}$ is the reduced mass of ions or electrons, v is the relative velocity of the scattered test particle, $b_\perp = |Z_\alpha||Z_\beta|e^2/(m_{\alpha\beta}v^2)$, $Z_e = -1$, $Z_i = 1$, and $\Lambda_{\alpha\beta}$ is the Coulomb logarithm.

The Coulomb logarithm based on the effective interaction potential of particles is determined by the scattering angle of pair collisions. Introducing the center of mass in the collision process, the Coulomb logarithm is written as[21,30,31]

$$\Lambda_{\alpha\beta} = \frac{1}{b_\perp^2} \int_0^\infty \sin^2 \left(\frac{\theta_c}{2} \right) b \, db, \tag{7}$$

where the center-of-mass scattering angle θ_c can be obtained from the formula[30]

$$\theta_c = \pi - 2b \int_{r_0}^\infty \frac{dr}{r^2} \left(1 - \frac{\Phi_{\alpha\beta}(r)}{E_c} - \frac{b^2}{r^2} \right)^{-1/2}. \tag{8}$$

In Equation 8, $\Phi_{\alpha\beta}(r)$ is the interaction potential, and r_0 is the distance of the closest approach for a given impact parameter b:

$$1 - \frac{\Phi_{\alpha\beta}(r_0)}{E_c} - \frac{b^2}{r_0^2} = 0. \tag{9}$$

It is known that, in order to correctly describe static and dynamic properties of plasmas, the collective screening effect is to be taken into account. In this work, the dense plasma, for which quantum effects at short distances must be taken into account, is considered. Further, the effective interaction potential including both charge screening at large distances and quantum effects at short distances are used:[25–27]

$$\Phi_{\alpha\beta}(r) = \frac{e^2 Z_\alpha Z_\beta}{r \lambda_{ee}^2 \gamma^2 \sqrt{1 - (2k_D/\lambda_{ee}\gamma^2)^2}} \left[\left(\frac{1 - \lambda_{ee}^2 B^2}{1 - \lambda_{\alpha\beta}^2 B^2} \right) \exp(-rB) - \left(\frac{1 - \lambda_{ee}^2 A^2}{1 - \lambda_{\alpha\beta}^2 A^2} \right) \exp(-rA) \right] +$$
$$+ \frac{Z e^2 \exp(-r/\lambda_{\alpha\beta})}{r(1 + C_{\alpha\beta})}, \tag{10}$$

where $A^2 = \frac{\gamma^2}{2}\left(1 + \sqrt{1 - \left(\frac{2k_D}{\lambda_{ee}\gamma^2}\right)^2}\right)$, $B^2 = \frac{\gamma^2}{2}\left(1 - \sqrt{1 - \left(\frac{2k_D}{\lambda_{ee}\gamma^2}\right)^2}\right)$, $C_{\alpha\beta} = (k_D^2\lambda_{\alpha\beta}^2 - k_i^2\lambda_{ee}^2)/(\lambda_{ee}^2/\lambda_{\alpha\beta}^2 - 1)$, $\gamma^2 = k_i^2 + 1/\lambda_{ee}^2$, $\lambda_{ee}^2 = -b_1/4k_F^2$, $k_{De} = k_Y$, $k_D^2 = k_{De}^2 + k_i^2$, $k_i^2 = 4\pi n_i e^2/k_B T_i$, $b_1 = \theta^{-1}I_{-3/2}(\eta)/(3I_{-1/2}^2(\eta))$, with I_ν being the Fermi integral of the order ν, and $\lambda_{\alpha\beta} = \hbar/\sqrt{2\pi m_{\alpha\beta}k_B T_{\alpha\beta}}$ is the characteristic thermal de Brogile wavelength. In nonisothermal plasmas, a characteristic temperature $T_{\alpha\beta}$ appears.[32,33] In Ref. [32], it was shown that for a correct description of two-temperature plasma properties, the temperature may be expressed in the form $T_{\alpha\beta} = \sqrt{T_\alpha T_\beta}$. The effective potential 10 can be used for non-isothermal as well as isothermal plasmas. It is important to note that the effective potential 10 for the case of ion–ion interaction agrees with that of Ref. [34].

3 | RESULTS AND DISCUSSION

In this section, we consider the results of investigation of the dynamic properties of dense plasmas based on the Coulomb logarithm using the effective potential 10. Stopping processes in a dense plasma are of significant interest in various fields of science and technology (plasma physics, ICF, physics of warm dense matter, etc.).[35,36] In particular, intensive studies of ICF require more reliable information about the dynamic characteristics, that is, the stopping power and temperature relaxation. Let us consider a dense DT plasma particles interacting through the effective potential 10.

The quality of description of the dynamic properties based on the effective potential 10 is checked by the comparison of the stopping power calculated using the combined model, T-matrix method and the first-order Born approximation with the data obtained using the effective electron–ion potential 10.

The stopping power obtained using the effective potential 10 and the results of calculations using the combined model, the first Born approximation, T-matrix model, dynamic random phase approximation (RPA), and PIC simulation are shown in Figure 1. The effective potential 10 correctly describes the stopping power at $v \lesssim v_{th}$, where $v_{th} = \sqrt{k_B T/m_e}$ is the electronic thermal velocity. The data obtained from the combined model are in agreement with the simulation data at velocities $v < 2\, v_{th}$. In the cases $Z = 5$ (Figure 1a) and $Z = 10$ (Figure 1b), at high velocities the effective potential 10 gives the results closer to the Born approximation. Moreover, from Figure 1 it can be concluded that the effective potential 10 provides a correct description of the stopping power at velocities $v \leq 1.5v_{th}$. In this velocity range, the effect of strong coupling between target and projectile is particularly important and the stopping power description in this range is particularly difficult. For instance, the T-matrix approach requires a rigorous solution of the quantum scattering problem and PIC simulation of the stopping power is known to be a time-consuming process. The effective interaction potential approach correctly describes the stopping power at low velocities including the region where the stopping power has its maximum, but fails to reproduce the result of the fully dynamical computation of the stopping power at $v > 2v_{th}$. On the other hand, such a fully dynamical method based on the direct use of the dynamical dielectric function from linear response theory essentially fails to provide reliable data on the stopping power at low projectile velocities, $v < 3v_{th}$. The region around $v \lesssim v_{th}$ is important for the correct calculation of the thermalization (temperature relaxation) time and, therefore, for the determination of the equilibrium plasma temperature in the case when a generated plasma has initially a non-isothermal state. It is important that the best theoretical result is provided by the combined scheme, where the T-matrix approach is used for low velocities and the dynamic RPA description is implemented at large projectile velocities. From the presented comparisons in Figure 1, we conclude that the employed effetive potential approach can be used for the fast and accurate computation of the stopping power in dense plasmas at low projectile velocities. Further, we use the effective potential approach for the analysis of the stopping power around its maximum, which is the most challenging region for theoretical considerations, at different plasma parameters.

In Figure 2a and b, we illustrate the energy dependence of the electron and ion components of the stopping power in a dense plasma at electron number density $n_e = 10^{26}$ cm^{-3} for different values of temperature. The plasma temperature is $T = 10$ divided by 30 keV, and the electron number density is $n_e = 10^{26}$ cm^{-3}, which is characteristic of plasmas for ICF shortly after ignition. The energy region lies between zero and α-particle energy $E_0 = 3.54$ MeV produced in the DT reaction. In this case, most of the α-particle energy is transferred to electrons. As shown in Figure 2, for ion projectiles, the energy loss to the electrons in the plasma dominates over that to the ions when the projectile energy becomes sufficiently large on the temperature scale. On the basis of the obtained data, the fractions of energy absorbed by an ion E_i and an electron E_e were estimated. The energy fractions transferred to electrons and ions calculated by the formulas 2 and 3 are $E_e = 3.38$ MeV and $E_i = 0.14$ MeV, respectively. Interestingly, the stopping power values around the maximum remain nearly constant when the temperature doubles from 10 to 20 keV, while the increase of temperature from 40 to 60 keV leads to the significant decrease in the stopping power around its maximum value.

In Figure 2b shows the stopping power by the present model, BPS (Bogomol'nyi–Prasad–Sommerfeld) theory,[29] and the average atom (AA) model.[37] The results obtained using the effective potential approach of this paper closer to those by Bin[37]
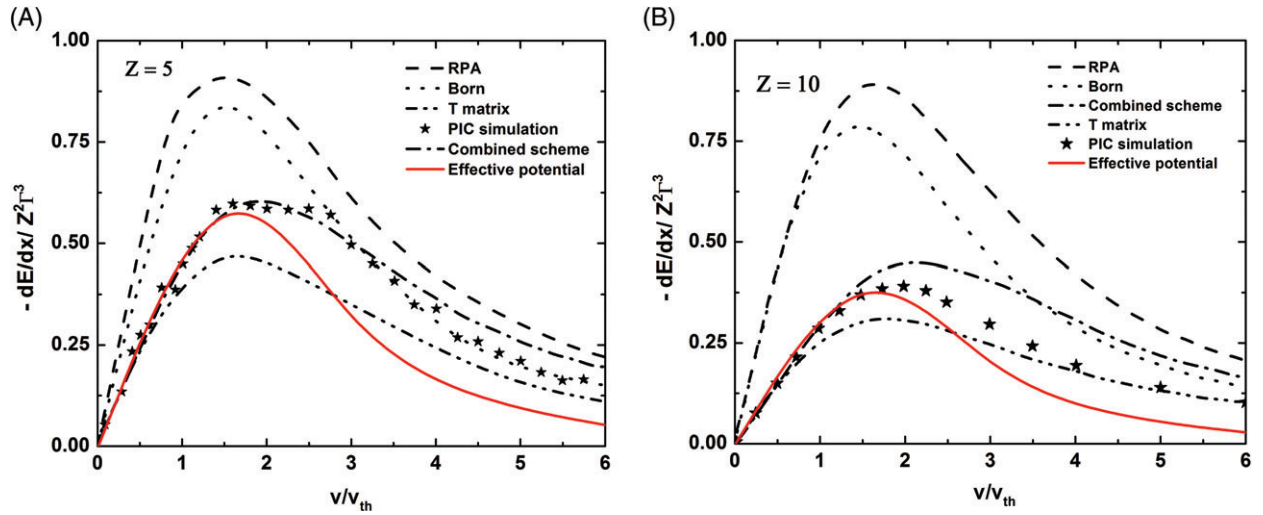
FIGURE 1 Stopping power obtained on the basis of the effective interaction potential 10 in comparison with the results of different theoretical approaches[19] for $Z = 5$ (a) and $Z = 10$ (b). The stopping power is given in units of $3k_BT/r_D$, where r_D is the Debye screening length, and $v_{\text{th}} = \sqrt{k_BT/m_e}$ is the thermal velocity
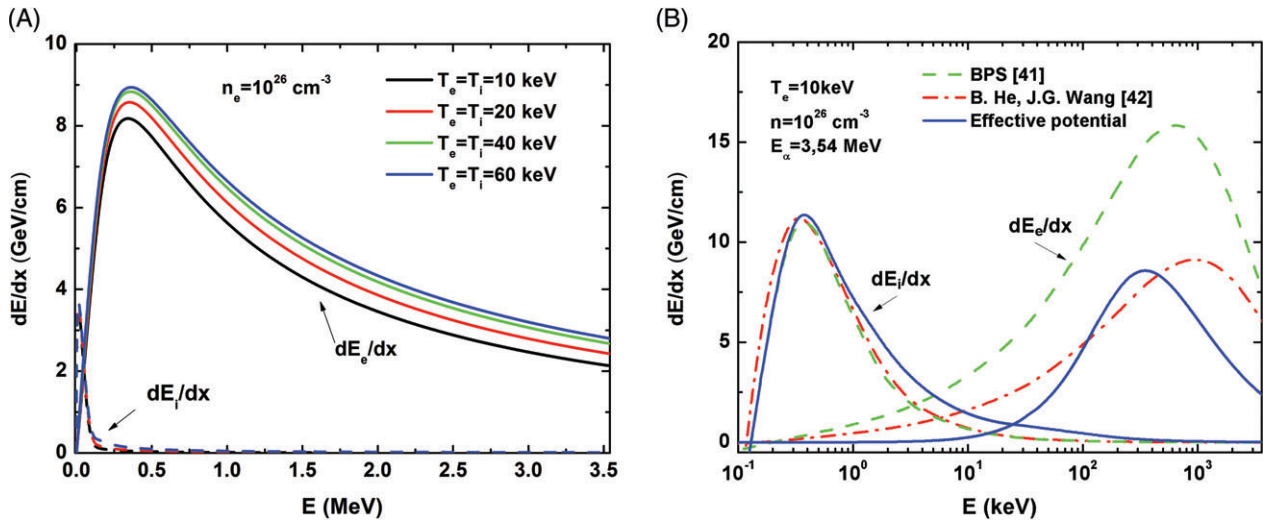

FIGURE 2 Stopping power of the projectile particle traversing a DT plasma as a function of the projectile energy, split into ion and electron contributions

rather than to the data from Ref. [29]. This indicates the importance of the electronic quantum effects, which are taken into account in Ref. [37]. The difference between our results and the result of Bin[37] is due to an inelastic scattering effect, which is included in Ref. [37], as the dense plasma of Au was considered. The latter is irrelevant when considering the case of a fully ionized dense DT plasma.

Figure 3 shows the α-particle range R_α in micrometers for the initial energy $E_0 = 3.54$ MeV as a function of the electron temperature T_e. The curves for different electron densities are labelled as follows: solid curves $n_e = 10^{26}$ cm^{-3}; dashed curves $n_e = 10^{25}$ cm^{-3}; dot-dashed curves $n_e = 10^{24}$ cm^{-3}. At the considered densities the α-particle range almost saturates at $T > $ keV after a dramatic increase at lower temperatures. It is worth noting that a smaller α-particle range is better for the efficient energy transfer from the α-particle to a plasma, meaning that an α-particle's initial energy deposition to a plasma is more effective at higher plasma densities.

Figure 4 shows the temperature relaxation of a helium ion ($Z = 2$) in a hydroge plasma with $T_e = T_i = 100$ eV and $n_e = 10^{24}$ cm^{-3} for two initial temperatures, that is, 10 and 1000 eV. The results are compared with the classical multi-component MD simulations[38] using a code based on the works of Hansen and McDonald[43] and Glosli et al.[44]. The obtained results agree with the results of the MD simulation. From Figure 4, the significant difference from the result obtained using the simpler Yukawa potential is seen. For instance, at the parameters indicated in Figure 4, the equilibrium value of the temperature calculated using the effective potential 10 is larger by 10 eV than that computed using the Yukawa potential. We note that the effective potential 10 agrees with the Yukawa potential if the electronic quantum non-locality (diffraction) effects are neglected. Therefore, an accurate description of the screening effect is highly important for the accurate description of the temperature equilibration in dense plasmas.
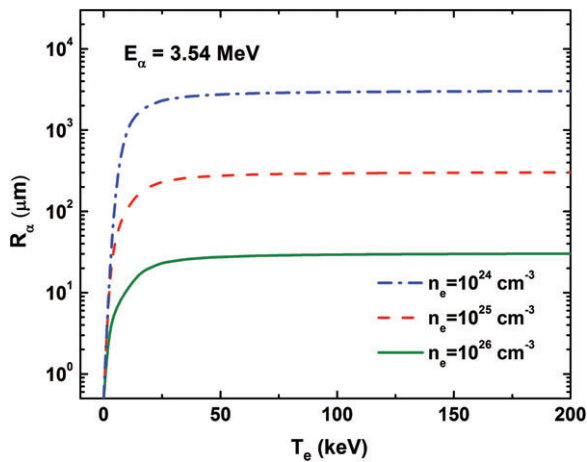
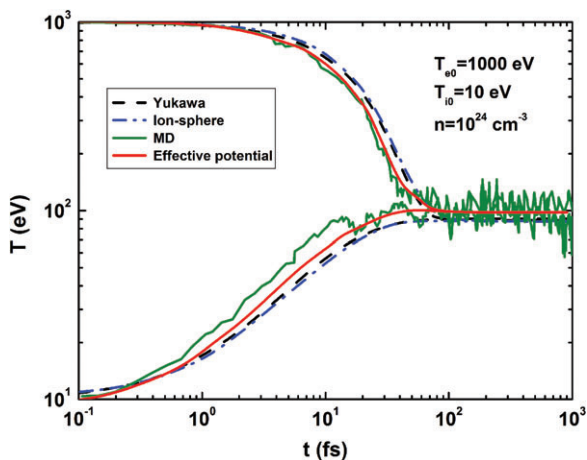**FIGURE 3** α-Particle range (in micrometers) as a function of the electron temperature

FIGURE 4 Comparison of the values of helium ion relaxation in hydrogen plasma for two initial energies $T_{i0} = 10$ eV and $T_{e0} = 1000$ eV with molecular dynamics (MD) simulations,[38] Yukawa potential,[39–41] and ion-sphere[42] potential

4 | CONCLUSION

The dynamic processes in dense DT plasmas were studied on the basis of the two-temperature effective interaction potentials taking into account quantum diffraction effects at short distances and screening at large distances. Although the used model is reliable only at relatively low projectile velocities, the important area around the maximum of the stopping power is adequately described. Therefore, this allowed us to study the dependence of the stopping power on plasma parameters and examine the sensitivity of the computed relaxation time and the corresponding equilibrium plasma temperature on the quality of the description of the screening effect in dense plasmas. The main findings are summarized as follows:

1. The stopping power in dense plasmas has non-monotonic dependence on the plasma temperature. At $T > 20$ keV, the stopping power at low velocities decreases with increase in the plasma temperature, while at 10 keV $< T < 20$ keV the stopping power does not show any significant change due to temperature variation.
2. A theoretically computed temperature equilibration in dense plasmas can be very sensitive to the approximation made in the description of the screening effect. Particularly, neglecting the electronic quantum non-locality can lead to a significant underestimation of the equilibrium temperature after thermalization. The reason for this is that the temperature relaxation is determined by the collisions with low ion velocities (relative to the electron thermal temperature). Therefore, the temperature equilibration in dense plasmas needs further study, implementing more involved theories for the description of the screening (e.g., see Ref. [45]).

REFERENCES

[1] V. E. Fortov, *Extreme States of Matter on Earth and in the Cosmos*, Springer, Berlin **2009**.

[2] V. E. Fortov, O. F. Petrov, O. S. Vaulina, R. A. Timirkhanov, *Phys. Rev. Lett.* **2012**, *109*, 055002.

[3] V. E. Fortov, A. V. Ivlev, S. A. Khrapak, A. G. Khrapak, G. E. Morfill, *Phys. Rep.* **2005**, *424*, 1.

[4] D. H. H. Hoffmann, A. Blazevic, P. Ni, O. Rosmej, M. Roth, N. A. Tahir, A. Tauschwitz, S. Udrea, D. Varentsov, K. Weyrich, Y. Maron, *Laser Part. Beams* **2005**, *23*, 47.

[5] B. Y. Sharkov, D. H. H. Hoffmann, A. A. Golubev, Y. Zhao, *Matter Radiat. Extremes* **2016**, *1*, 28.

[6] S. Kawata, T. Karino, A. I. Ogoyski, *Matter Radiat. Extremes* **2016**, *1*, 89.

[7] O. A. Hurricane, D. A. Callahan, D. T. Casey, P. M. Celliers, C. Cerjan, E. L. Dewald, T. R. Dittrich, T. Döppner, D. E. Hinkel, L. F. B. Hopkins, J. L. Kline, S. le Pape, T. Ma, A. G. MacPhee, J. L. Milovich, A. Pak, H. S. Park, P. K. Patel, B. A. Remington, J. D. Salmonson, P. T. Springer, R. Tommasini, *Nature* **2014**, *506*, 343.

[8] M. R. Gomez, S. A. Slutz, A. B. Sefkow, D. B. Sinars, K. D. Hahn, S. B. Hansen, E. C. Harding, P. F. Knapp, P. F. Schmit, C. A. Jennings, T. J. Awe, M. Geissel, D. C. Rovang, G. A. Chandler, G. W. Cooper, M. E. Cuneo, A. J. Harvey-Thompson, M. C. Herrmann, M. H. Hess, O. Johns, D. C. Lamppa, M. R. Martin, R. D. McBride, K. J. Peterson, J. L. Porter, G. K. Robertson, G. A. Rochau, C. L. Ruiz, M. E. Savage, I. C. Smith, W. A. Stygar, R. A. Vesey, *Phys. Rev. Lett.* **2014**, *113*, 155003.

[9] D. Casas, M. D. Barriga-Carrasco, J. Rubio, *Phys. Rev. E* **2013**, *88*, 033102.

[10] Y. V. Arkhipov, F. B. Baimbetov, A. E. Davletov, K. V. Starikov, *Phys. Scr.* **2001**, *63*, 194.

[11] Y. V. Arkhipov, A. B. Ashikbayeva, A. Askaruly, A. E. Davletov, I. M. Tkachenko, *EPL* **2013**, *104*, 35003-1.

[12] C. Deutsch, D. Leger, B. Tashev, *Laser Part. Beams* **2011**, *29*, 121.

[13] M. D. Barriga-Carrasco, *Phys. Rev. E* **2009**, *79*, 027401.

[14] M. D. Barriga-Carrasco, *Phys. Rev. E* **2010**, *82*, 046403.

[15] G. Belyaev, M. Basko, A. Cherkasov, A. Golubev, A. Fertman, I. Roudskoy, S. Savin, B. Sharkov, V. Turtikov, A. Arzumanov, A. Borisenko, I. Gorlachev, S. Lysukhin, D. H. H. Hoffmann, A. Tauschwitz, *Phys. Rev. E* **1996**, *53*, 2701.

[16] A. Golubev, M. Basko, A. Fertman, A. Kozodaev, N. Mesheryakov, B. Sharkov, A. Vishnevskiy, V. Fortov, M. Kulish, V. Gryaznov, V. Mintsev, E. Golubev, A. Pukhov, V. Smirnov, U. Funk, S. Stoewe, M. Stetter, H. P. Flierl, D. H. H. Hoffmann, J. Jacoby, I. Iosilevski, *Phys. Rev. E* **1998**, *57*, 3363.

[17] D. O. Gericke, M. Schlanges, *Phys. Rev. E* **1999**, *60*, 904.

[18] G. Zwicknagel, C. Toeper, P. G. Reinhardt, *Laser Part. Beams* **1995**, *13*, 311.

[19] D. O. Gericke, M. S. Murillo, M. Schlanges, *Phys. Rev. E* **2002**, *65*, 036418.

[20] K. Shibata, A. Sakumi, *Nucl. Instrum. Methods Phys. Res. A* **2001**, *464*, 225.

[21] T. S. Ramazanov, S. K. Kodanova, Z. A. Moldabekov, M. K. Issanova, *Phys. Plasmas* **2013**, *20*, 112702.

[22] T. S. Ramazanov, Z. A. Moldabekov, M. T. Gabdullin, *Phys. Rev. E* **2015**, *92*, 023104.

[23] S. K. Kodanova, T. S. Ramazanov, M. K. Issanova, G. N. Nigmetova, Z. Moldabekov, *Contrib. Plasma Phys.* **2015**, *55*, 271.

[24] M. K. Issanova, S. K. Kodanova, T. S. Ramazanov, N. K. Bastykova, Z. A. Moldabekov, C.-V. Meister, *Laser Part. Beams* **2016**, *34*, 457.

[25] Z. Moldabekov, T. Schoof, P. Ludwig, M. Bonitz, T. Ramazanov, *Phys. Plasmas* **2015**, *22*, 102104.

[26] T. S. Ramazanov, Z. A. Moldabekov, M. T. Gabdullin, *Phys. Plasmas* **2016**, *23*, 042703.

[27] S. K. Kodanova, M. K. Issanova, S. M. Amirov, T. S. Ramazanov, A. Tikhonov, Z. A. Moldabekov, *Matter Radiat. Extremes* **2018**, *3*, 40.

[28] M. Mahdavi, T. Koohrokhi, *Phys. Rev. E* **2012**, *85*, 016405.

[29] L. S. Brown, D. L. Preston, R. L. Singleton Jr.. , *Phys. Rev. E* **2012**, *86*, 016406.

[30] C. A. Ordonez, M. I. Molina, *Phys. Plasmas* **1994**, *1*, 2515.

[31] T. S. Ramazanov, S. K. Kodanova, *Phys. Plasmas* **2001**, *8*, 5049.

[32] P. Seuferling, J. Vogel, C. Toepffer, *Phys. Rev. A* **1989**, *40*, 323.

[33] R. Bredow, T. Bornath, W. D. Kraeft, R. Redmer, *Contrib. Plasma Phys.* **2013**, *53*, 276.

[34] L. G. Stanton, M. S. Murillo, *Phys. Rev. E* **2015**, *91*, 033104.

[35] S. Atzeni, J. Meyer-ter-Vehn, *The Physics of Inertial Fusion: Beam Plasma Interaction, Hydrodynamics, Hot Dense Matter*. International Series of Monographs on Physics, Clarendon, Oxford **2004**.

[36] J. D. Lindl, *Inertial Confinement Fusion: The Quest for Ignition and Energy Gain Using Indirect Drive*, Springer-Verlag, New York **1998**.

[37] B. He, J. G. Wang, *Nucl. Fusion* **2013**, *53*, 093009.

[38] G. Faussurier, C. Blancard, M. Gauthier, *Phys. Plasmas* **2013**, *20*, 012705.

[39] R. M. More, *Adv. At. Mol. Phys.* **1985**, *21*, 305.

[40] G. Chabrier, *J. Phys.* **1990**, *51*, 1607.

[41] A. Y. Potekhin, G. Chabrier, D. Gilles, *Phys. Rev. E* **2002**, *65*, 036412.

[42] K. Scheibner, J. C. Weisheit, N. F. Lane, *Phys. Rev. A* **1987**, *35*, 1252.

[43] J. P. Hansen, I. R. McDonald, *Phys. Lett. A* **1983**, *97*, 42.

[44] J. N. Glosli, F. R. Graziani, R. M. More, M. S. Murillo, F. H. Streitz, M. P. Surh, L. X. Benedict, S. Hau-Riege, A. B. Langdon, R. A. London, *Phys. Rev. E* **2008**, *78*, 025401(R).

[45] Z. A. Moldabekov, S. Groth, T. Dornheim, M. Bonitz, T. S. Ramazanov, *Contrib. Plasma Phys.* **2017**, *57*, 532.